nature genetics

Mutations in *VPS33B*, encoding a regulator of SNARE-dependent membrane fusion, cause arthrogryposis–renal dysfunction–cholestasis (ARC) syndrome

Paul Gissen[1,2], Colin A Johnson[1], Neil V Morgan[1], Janneke M Stapelbroek[3], Tim Forshew[1], Wendy N Cooper[1], Patrick J McKiernan[2], Leo W J Klomp[4], Andrew A M Morris[5], James E Wraith[5], Patricia McClean[6], Sally A Lynch[7], Richard J Thompson[8], Bryan Lo[9], Oliver W Quarrell[10], Maja Di Rocco[11], Richard C Trembath[12], Hanna Mandel[13], S Wali[14], Fiona E Karet[15], A S Knisely[8], Roderick H J Houwen[3], Deirdre A Kelly[2] & Eamonn R Maher[1]

ARC syndrome (OMIM 208085) is an autosomal recessive multisystem disorder characterized by neurogenic arthrogryposis multiplex congenita, renal tubular dysfunction and neonatal cholestasis with bile duct hypoplasia and low gamma glutamyl transpeptidase (gGT) activity. Platelet dysfunction is common. Affected infants do not thrive and usually die in the first year of life[1–5]. To elucidate the molecular basis of ARC, we mapped the disease to a 7-cM interval on 15q26.1 and then identified germline mutations in the gene *VPS33B* in 14 kindreds with ARC. *VPS33B* encodes a homolog of the class C yeast vacuolar protein sorting gene, *Vps33*, that contains a Sec1-like domain important in the regulation of vesicle-to-target SNARE complex formation and subsequent membrane fusion[6–9].

We identified 15 kindreds including 29 individuals affected with ARC syndrome. First, we excluded linkage to the candidate genes *ATP8B1* and *ABCB11* (ref. 10), which are implicated in other disorders that cause neonatal cholestasis with low gGT activity. We then carried out a genome-wide linkage scan using the Affymetrix 10K SNP chip[11–14] in seven affected individuals from six consanguineous kindreds with ARC. This scan identified eight regions of extended homozygosity shared by all affected individuals. We analyzed these regions further by typing microsatellite markers in 64 individuals from 14 consanguineous families (**Fig. 1** and **Supplementary Fig. 1**

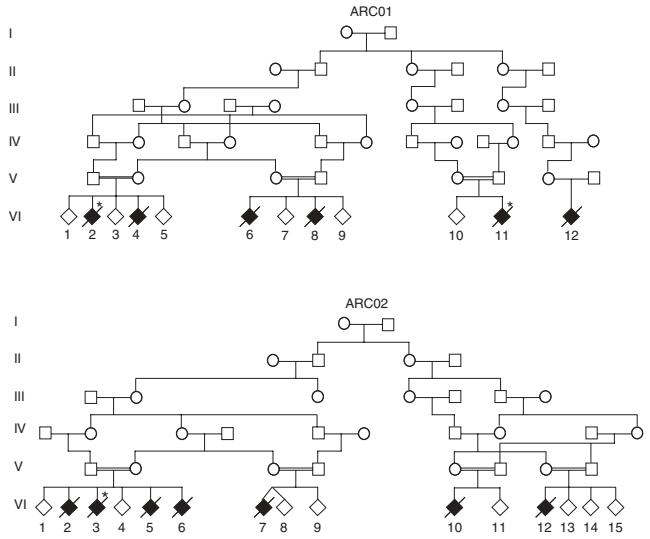

Figure 1 Pedigrees for the two largest kindreds (ARC01 and ARC02). Pedigrees for families ARC03–ARC15 are provided in **Supplementary Figure 1** online. The asterisks indicate individuals whose DNA was used for the genome-wide SNP linkage scan.

[1]Section of Medical and Molecular Genetics, University of Birmingham, Edgbaston, Birmingham B15 2TT, UK. [2]The Liver Unit, Birmingham Children's Hospital, Birmingham, B4 6NH, UK. [3]Department of Pediatric Gastroenterology, University Medical Center, Utrecht, The Netherlands. [4]Department of Metabolic and Endocrine diseases, University Medical Center, Utrecht, The Netherlands. [5]Willink Biochemical Genetics Unit, Royal Manchester Children's Hospital, Hospital Road, Pendlebury, Manchester M27 4HA, UK. [6]Department of Paediatrics, St. James's Hospital, Leeds LS9 7TF, UK. [7]Institute of Human Genetics, International Centre for Life, Central Parkway, Newcastle NE1 3BZ, UK. [8]Institute of Liver Studies, King's College Hospital, London SE5 9RS, UK. [9]The Hospital for Sick Children Division of Clinical and Metabolic Genetics, 555 University Avenue, Toronto, Ontario M5G 1X8, Canada. [10]Department of Clinical Genetics, Sheffield Children's Hospital, Sheffield S10 2TH, UK. [11]II Pediatric Unit, Gaslini Institute, Largo Gaslini 5, 16147 Genoa, Italy. [12]Division of Medical Genetics, Departments of Genetics and Cardiovascular Sciences, University of Leicester, Leicester LE1 7RH, UK. [13]Metabolic Disease and Pediatric Gastroenterology and Nutrition Units, Department of Pediatrics, Rambam Medical Center, Technion–Israel Institute of Technology, Bruce Rappaport Faculty of Medicine, Haifa, Israel. [14]Department of Pediatrics, Riyadh Armed Forces Hospital, Riyadh, Saudi Arabia. [15]Departments of Medical Genetics and Nephrology, University of Cambridge, Cambridge Institute for Medical Research, Box 139, Addenbrooke's Hospital, Cambridge, CB2 2XY, UK. Correspondence should be addressed to E.R.M. (E.R.Maher@bham.ac.uk).

Published online 28 March 2004; doi:10.1038/ng1325

online). We confirmed a region of homozygosity between markers *D15S816* and *D15S655* on chromosome 15q26.1 with a maximum two-point lod score of 9.8 for $\theta = 0$ at marker *D15S652*. Fine-mapping with additional markers developed from the draft human genome sequence narrowed the candidate region to an interval of 0.7 Mb between markers *D15S127* and *D15S158* (**Supplementary Fig. 1** online).

We constructed an *in silico* genomic map of the region using public databases (**Fig. 2a**). We then prioritized genes for mutation screening on the basis of putative function and expression patterns. In view of the multiorgan involvement in ARC, we selected three ubiquitously expressed genes (*FURIN*, *MAN2A2* and *VPS33B*) for mutation analysis by direct sequencing of DNA from four consanguineous individuals with ARC. We detected no germline mutations in *FURIN* or *MAN2A2* but identified two nonsense mutations (1593C→T, R532X and 1311C→T, R438X) in *VPS33B* in the four probands. In each case, the *VPS33B* mutation segregated with disease status in the family and was not present in 132 ethnically matched control chromosomes. We then identified germline *VPS33B* mutations in 10 of 11 additional probands (**Table 1**). Each of these mutations segregated with the disease status, and none was present in the control cohort. We identified three nonsense, one frameshift and four splice-site mutations, all of which are predicted to impair the function of the *VPS33B* gene product.

We also identified a homozygous missense mutation (resulting in the amino acid substitution L30P) in conserved region (**Fig. 2b**,**c**), which may represent a dileucine motif. This motif is thought to be important for intracellular localization and is a sorting signal present in endosomal-lysosomal targeting proteins[15,16]. Affected children in 13 consanguineous families were homozygous with respect to a *VPS33B* mutation, and one affected child in a nonconsanguineous family was a compound heterozygote. We detected no mutations in one individual despite sequencing all exons with intron-exon boundaries. Seven apparently unrelated families of Pakistani origin shared a 1311C→T nonsense mutation. Inspection of the genotype data in these families provided evidence for a common haplotype, suggestive of a founder effect.

Immunostaining of liver biopsy samples from six individuals with ARC using a polyclonal antibody against carcinoembryonic antigen (CEA), a hepatocyte plasma-membrane glycoprotein normally present only at the canaliculus, showed marked disturbance in CEA localization, with a uniform distribution at the canalicular and basolateral plasma membranes and widespread intracellular immunostaining (**Fig. 3a**). We also observed that other plasma membrane proteins were not restricted to normal apical (polarized) domains in tissue from individuals with ARC, by immunostaining specimens with a polyclonal antibody against gGT and with a monoclonal antibody against dipeptidyl peptidase CD26 (**Fig. 3b**; anti-CEA and anti-gGT, liver and kidney; anti-CD26, kidney)[17]. This pattern of disordered antigen expression

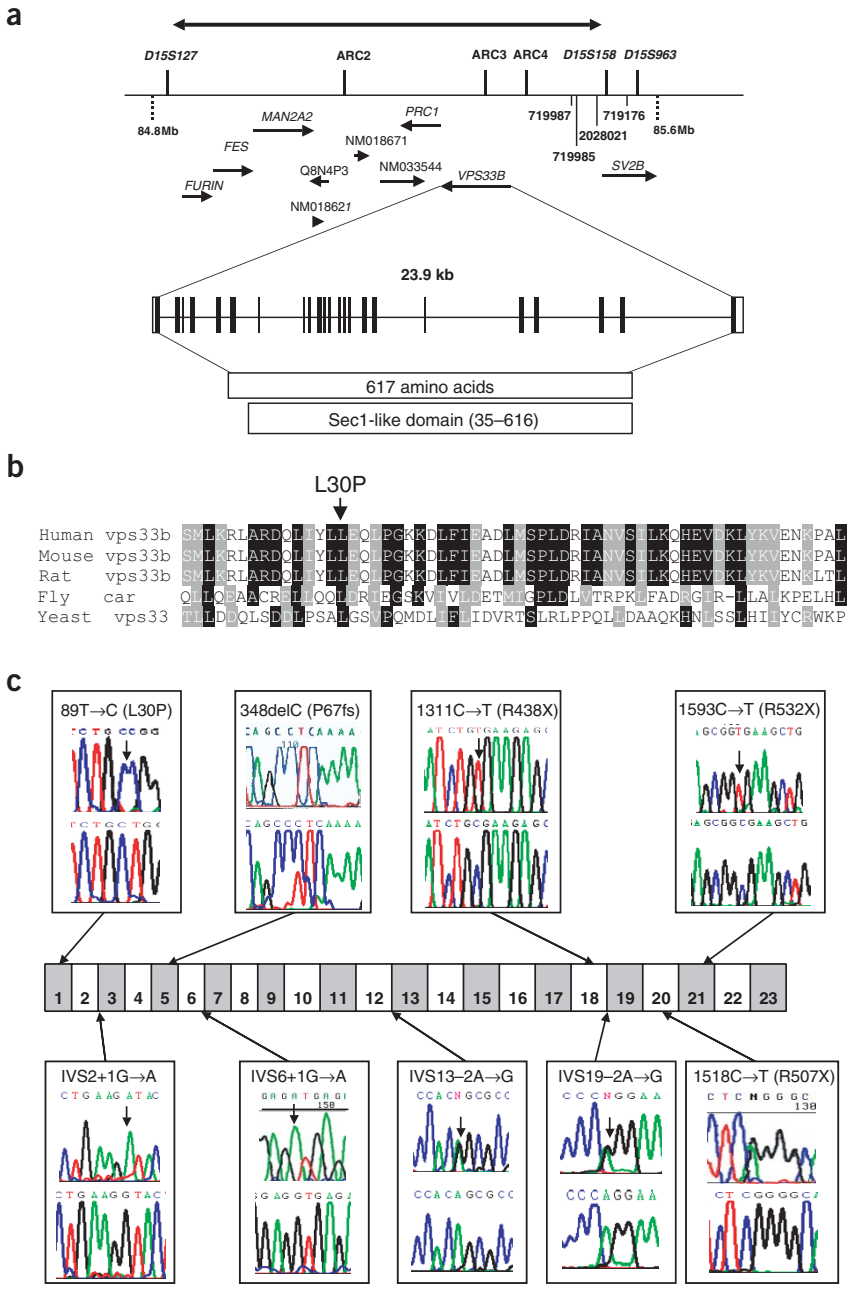

Figure 2 Mapping of the ARC locus and mutation analysis of *VPS33B*. (**a**) ARC candidate gene region as annotated by Ensembl, with arrows indicating the location of genes on the positive or negative strands. (**b**) Alignment of *VPS33B* homologs from five different species. Leu30 is conserved among mammals, and the dileucine motif may represent a targeting signal. (**c**) Mutations in individuals with ARC syndrome. Mutations in *VPS33B* are shown by sequence traces (nucleotide and amino acid exchange) from affected individuals (top) and healthy controls (bottom). Arrows indicate the exon or exon-intron boundary in which each mutation was found. The mutation IVS19–2A→G mutation is shown in a heterozygous carrier. The mutation 1518C→T mutation is shown in the reverse read.

Table 1 Mutations in *VPS33B* in individuals with ARC syndrome

Pedigree number	Reference for clinical details	Ethnic origin	Nucleotide alterations	Alterations in coding sequence	Exon	Status	Parental consanguinity
ARC01	3	Pakistani	1593C→T	R532X	21	Hom	Yes
ARC02	4	Pakistani	1311C→T	R438X	18	Hom	Yes
ARC03		Pakistani	1311C→T	R438X	18	Hom	Yes
ARC04	3	Pakistani	1311C→T	R438X	18	Hom	Yes
ARC05		Pakistani	1311C→T	R438X	18	Hom	Yes
ARC06		Pakistani	1311C→T	R438X	18	Hom	Yes
ARC07	4	Pakistani	1311C→T	R438X	18	Hom	Yes
ARC08	3	Pakistani	1311C→T	R438X	18	Hom	Yes
ARC09	3	Pakistani	89T→C	L30P	1	Hom	Yes
ARC10	2	Southern European	IVS2+1G→A		2+1	Hom	Yes
ARC11		Arab	348delC	S116fsX136	5	Hom	Yes
ARC12		Arab	ND				Yes
ARC13		Arab	IVS6+1G→A		6+1	Hom	Yes
ARC14	5	Arab	IVS19–2A→G		19–2	Hom	Yes
ARC15		Southern European	1518C→T, IVS13–2A→G	R507X	20, 13–2	Het, Het	No

Nucleotides are numbered from A of the initiation codon (ATG). Het, heterozygous; hom, homozygous; ND, not detected; fs, frameshift; del, deletion; X, stop.

was not seen in age-matched normal kidney samples, in age-matched normal liver samples or in liver samples from individuals with other forms of low-gGT cholestasis (*e.g.*, familial hypercholanemia, *ABCB11* disease) and was consonant with failure of membrane polarization or abnormal trafficking of surface-expressed proteins.

The function of a VPS33B protein has not been studied previously in humans, although human VPS33B is ubiquitously expressed in fetal and adult tissues[6]. The yeast homolog Vps33, a class C vacuolar protein sorting protein, is required for vacuolar biogenesis and has a key role in the late stages of protein trafficking from Golgi to vacuole. Yeast mutants of the class C vps complex (consisting of *Vps11*, *Vps16*, *Vps18*, *Vps33* and *Vps39*) have severe intracellular acid-base imbalance, amino acid pool deficiency and temperature-sensitive growth failure[18]. In fruit flies, a hypomorphic allele of *Vps33* causes the carnation eye-color mutant. The carnation gene product (car) localizes to endosomal compartments and is a homolog of Sec1p-like regulators of membrane fusion[19]. The only previously known mammalian class C vps complex mutant is the buff (*bf*) mouse, caused by a mutation in mouse *Vps33a*. The *bf* mouse, which has been suggested as an animal model for Hermansky-Pudlak syndrome, is characterized by hypopigmentation and a mild platelet storage pool deficiency but no clear abnormality of lysosomal function[20]. Platelet-function abnormalities described in ARC syndrome could result from abnormal organelle biogenesis, like those in the *bf* mouse[1].

VPS33B contains a Sec1-like domain and belongs to the family of SM (Sec1/Munc18-like) proteins that bind tightly to members of the syntaxin family of target SNAREs (soluble N-ethylmaleimide-sensitive factor attachment protein receptor or SNAP receptor proteins). SM proteins may alter interdomain interactions in target SNAREs and influence vesicle-to-target SNARE complex assembly[21–23]. To determine whether VPS33B might interact specifically with syntaxin 7 (ref. 24), we carried out coimmunoprecipitation experiments with an antibody to syntaxin 7 but found no evidence for coimmunoprecipitation of VPS33B and syntaxin 7 (data not shown).

Overexpression of mammalian class C VPS protein homologs (*e.g.*, VPS18 and VPS39) in human cells causes perinuclear clustering of late endosomes and lysosomes[25–27]. This is consistent with a role for these class C complex components in the recruitment of these membrane-bound organelles for the fusion events required for endo- or exocytosis and secretion. We therefore investigated whether overexpression of VPS33B would have a similar effect. We transfected renal cell carcinoma (RCC4) cell lines with wild-type VPS33B labeled with green fluorescent protein (GFP). We detected

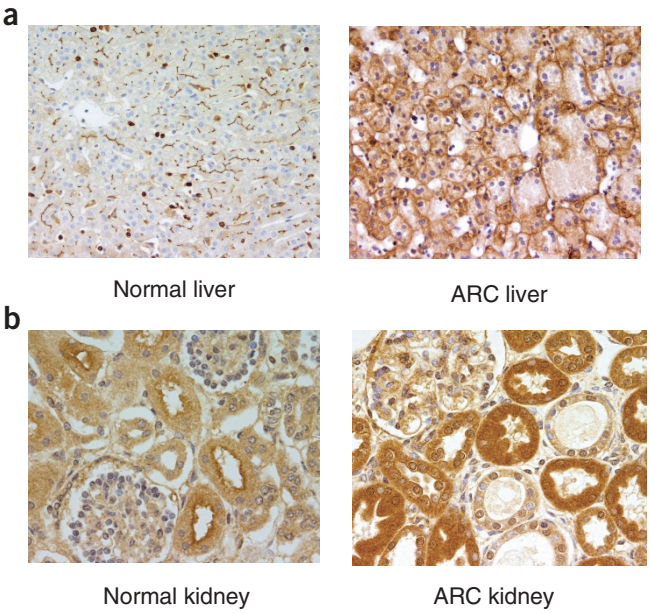

Figure 3 Immunostaining of liver and kidney biopsy samples from individuals with ARC. (**a**) Immunostaining with polyclonal antibody to CEA (original magnification, 200). Formalin-fixed, paraffin-embedded liver from an individual with ARC from family ARC09. Distribution of CEA is markedly disturbed. In the age-matched control, marking for CEA is limited to the canalicular membrane. In the individual with ARC, CEA is seen in cytoplasm and at basolateral membranes as well. (**b**) Immunostaining with antibody to CD26 (original magnification, 400). Formalin-fixed, paraffin-embedded kidney from an individual with ARC from family ARC01 and an age-matched control. Loss of brush-border accentuation is apparent in the individual with ARC.

clustering of late endosomal-lysosomal organelles in 10 of 20 GFP-VPS33B-positive RCC4 cells but in none of 20 GFP-VPS33B-negative cells ($P < 0.0004$; **Fig. 4a**,**b**). Transfection with a truncated GFP-VPS33B protein did not induce clustering (data not shown). To investigate the intracellular localization of human VPS33B, we expressed GFP-labeled full-length and truncated VPS33B fusion proteins in an RCC4 cell line. We observed diffuse fluorescence and punctate accumulations in the cytoplasm. By real-time Richardson microscope imaging, we observed that punctate staining of GFP-labeled wild-type VPS33B coincided with vesicle-like structures, and further investigation indicated that wild-type VPS33B (but not truncated VPS33B) colocalized with LAMP1, a marker for late endosomes and lysosomes (**Fig. 4b**). Similar experiments with GM130 (a marker for the trans-Golgi network) and EEA1 (a marker for early endosomes) did not show evidence of colocalization with wild-type VPS33B (**Fig. 4c**,**d**).

Our intracellular localization findings are consistent with data on the role of VPS33B homologs in yeast and fruit flies and implicate VPS33B in the regulation of intracellular protein trafficking. Such a role would be consistent with the widespread organ dysfunction in ARC syndrome. Platelet dysfunction could be attributed to abnormal biosynthesis or exocytosis of alpha granules. Immunohistochemical analysis has also suggested that abnormal protein trafficking may be involved in ARC, including focal deficiency of gGT at the canalicular membrane. ARC is characterized by low serum gGT activity despite cholestasis. This may reflect reduced availability of gGT for elution into bile and thence into plasma[3,17]. Renal tubular acidosis is another feature of ARC. It can also be caused by inherited mutations that result in erroneous targeting of the polytopic chloride–bicarbonate exchanger AE1 protein to apical as well as the basolateral surface of the renal tubular cell[28].

We showed that mutations in *VPS33B* cause ARC syndrome. The clinical features of renal tubular abnormalities, cholestasis, hypotonia and platelet storage pool deficiency are consistent with abnormal intracellular protein trafficking and defective membrane fusion mechanisms in the kidneys, liver, nervous system and platelets. The association of mutations in *VPS33B* with human disease provides a model for investigating the role of the ubiquitous SNARE-related pathways in human disease and normal cellular function.

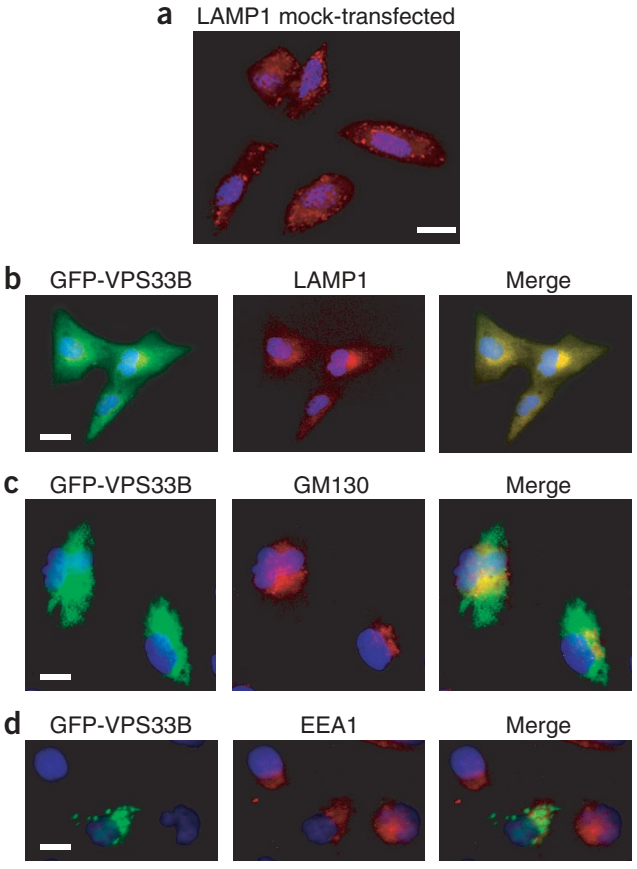

Figure 4 Intracellular localization and overexpression of VPS33B. (**a**) No clustering of organelles is apparent in mock-transfected cells. (**b**) Wild-type VPS33B (but not truncated VPS33B) colocalizes with LAMP1. Juxtanuclear clustering of late endosomes and lysosomes is detected by an antibody to LAMP1, labeled in red, with cells expressing GFP-VPS33B fusion protein in green. (**c**,**d**) No colocalization of wild-type VPS33B (green) is apparent with antibodies to either GM130 or EEA1 (red). Scale bars, 10 m.

METHODS

Affected individuals and families. Eight of the 15 families investigated have been described previously and all have a characteristic ARC phenotype (**Table 1**) with arthrogryposis multiplex congenita, renal tubular dysfunction and cholestasis with normal gGT activity. We obtained informed consent from all participating families, and the study was approved by the local research ethics committees. We extracted DNA from blood, lymphoblastoid and fibroblast cell lines, liver biopsy paraffin blocks and neonatal blood spots using standard methods. We used anonymized healthy laboratory control samples to assess population frequencies of DNA variants.

Genome-wide scan and fine-typing of the candidate regions. We genotyped seven individuals with ARC (shown in **Fig. 1** and **Supplementary Fig. 1** online) for 10,000 single-nucleotide polymorphisms (SNPs) at an average genetic distance of 1 cM, using the Affymetrix 10K SNP chip (MRC GeneService). We further investigated regions of shared homozygosity of >1 cM genetic distance and >4 homozygous contiguous SNPs by genotyping fluorescently labeled microsatellite markers from the candidate regions. We identified suitable markers using public genome databases and the deCODE, Marshfield and Généthon genetic maps. We designed new microsatellite markers from the ARC region using the chromosome 15 draft human genome sequence. We amplified DNA from affected individuals by PCR with microsatellite markers as described previously[11]. We separated PCR products by electrophoresis on an ABI 377 DNA Analyser and analyzed them with Genescan v3.1.2 and Genotyper v2.5.2 software (Applied Biosystems). We calculated two-point lod scores for 11 affected individuals and their parents using the MLINK program in the LINKAGE (version 5.1) software package.

Mutation analysis. We designed primers flanking all exons of *VPS33B*, *MAN2A2* and *FURIN* from the genomic sequence (primer sequences are available on request), carried out direct sequencing using the dideoxy chain termination method on either ABI 3700 or ABI 377 DNA Analysers and analyzed sequences using Chromas software. All mutations were verified bidirectionally.

Expression vectors. We obtained human *VPS33B* cDNA by RT-PCR amplification from total RNA of a normal healthy subject. Forward primers included the start codon, and reverse primers contained the native stop codon (primer sequences are available on request). We also created truncated *VPS33B* constructs to mimic the effect of the R438X mutation found in the Pakistani family (primer sequences are available on request). We designed primers from the human RefSeq sequence of *VPS33B*. Forward primers contained an *Eco*RI restriction site, and reverse primers contained *Bam*HI or *Kpn*I sites to allow subcloning of the cDNA fragments into the pEGFP-C2 or the pCMV-HA vectors (BD Biosciences Clontech), respectively.

Cells and antibodies. We grew human embryonic kidney (HEK293) and adult RCC4 cells in Dulbecco's minimal essential medium supplemented with 5%

fetal calf serum (Sigma-Aldrich). We obtained antibodies against syntaxin-7 (Santa-Cruz Biotechnology), LAMP-1 (Developmental Studies Hybridoma Bank, University of Iowa), EEA1 and GM130 (BD Biosciences) commercially. We obtained tetramethyl rhodamine isothiocyanate–conjugated goat antibodies to mouse and rabbit immunoglobulins for immunofluorescence microscopy and mouse monoclonal antibody to hemagglutinin for immunoprecipitation from Sigma-Aldrich. We obtained polyclonal antibody to CEA (DakoCytomation) and monoclonal antibody to CD26 (Stratech Scientific) commercially. Polyclonal antibody to gGT was a gift from M.H. Hanigan (Department of Cell Biology, University of Oklahoma Health Science Center, Oklahoma City, Oklahoma, USA). Tissue biopsy specimens studied were formalin-fixed and paraffin-embedded.

Transient transfection and immunofluorescence. For transient transfection experiments, we grew RCC4 and HEK293 cells on glass cover slips to ~80% confluence and transfected them with 500 ng of plasmid DNA (pEGFP vector, and pEGFP+VPS33B(1-617) or pEGFP+VPS33B(1-438) constructs) using Effectene reagent (Qiagen GmbH) for 24 h. We then removed transfection complexes and allowed cells to grow for another 24 h in normal medium. We washed RCC4 cells in phosphate-buffered saline (PBS), fixed them in 4% paraformaldehyde in PBS for 30 min and permeabilized them in PBST buffer (PBS, 10% (v/v) normal swine serum, 0.1% (v/v) Tween 20). We detected endogenous syntaxin-7, LAMP-1, GM130 and EEA1 using antibodies diluted 1:100 in PBST. We detected primary antibodies using tetramethyl rhodamine isothiocyanate–conjugated antibodies to goat or mouse IgG diluted 1:100 in PBST. All antibodies were applied at room temperature in a moist chamber. Finally, we applied antifade (Vectashield, Vector Laboratories) containing DAPI (2 g ml^{-1}) and visualized images with a Photometrics SenSys KAF 1400-G2 CCD fitted to a Zeiss Axioplan fluorescence microscope. We captured images using SmartCapture 2 software (Digital Scientific) running on a Macintosh G4 computer.

SDS-PAGE and western blotting. We prepared polyacrylamide gels containing SDS and used them to separate products as described elsewhere[29]. Western blots used standard blocking buffer (TBST; 50 mM Tris-HCl (pH 7.5), 150 mM NaCl, 0.05% (v/v) Tween 20) containing 5% (w/v) nonfat powdered dried milk (Marvel) as described elsewhere[29]. In general, we used rabbit polyclonal antisera for immunodetection, with final dilutions between 1:200 and 1:1,000. We used a peroxidase-conjugated secondary antibody for detection by enhanced chemiluminescence (Amersham Biosciences).

Immunoprecipitation of immunocomplexes. We prepared whole-cell extracts from HEK293 cells transiently transfected with pCMV-HA vector and pCMV-HA+VPS33B(1-617) or pCMV-HA+VPS33B(1-438) constructs. We scraped cells into PBS, washed them and resuspended them in lysis buffer (50 mM Tris (pH 7.5), 150 mM NaCl, 0.5 mM EDTA, 0.5 mM EGTA, 0.02% (w/v) NaN_3, 1.0% (v/v) Igepal C630 (Sigma-Aldrich), 10% (v/v) glycerol and a protease inhibitor cocktail for mammalian cell extracts from Sigma-Aldrich). We incubated the cell suspension on ice for 30 min with gentle stirring, sonicated it on ice and clarified it by centrifuging at 13,000*g* for 5 min. We processed the supernatant for immunoprecipitation using 5 g of purified mouse monoclonal antibody to hemagglutinin or antibody to syntaxin7 coupled to protein G– or protein A–sepharose beads (Amersham Biosciences)[30].

GenBank accession numbers. *Homo sapiens* chromosome 15 genomic contig used to generate new microsatellite markers, NT_010274.15; *H. sapiens VPS33B*, NM_018668; *Drosophila melanogaster Vps33* homolog *car*, NM_078686; *Mus musculus Vps33a*, NM_029929; *Saccharomyces cerevisiae vps33*, M34638; *M. musculus Vps33b*, BC034170.

Note: Supplementary information is available on the Nature Genetics website.

ACKNOWLEDGMENTS
We thank all the families for participation in research; M. Bingham and A. Dearlove for SNP genotyping; F. MacDonald, G. Gray and others for help in DNA extraction and storage of materials; P. Luzio, A. Dallol and D. White for discussions; and A. Barlow and Improvision UK for help with Richardson microscopy. This research was supported by 'Children Living with Inherited Metabolic diseases' registered UK charity, the Birmingham Children's Hospital Research Foundation and the Wellcome Trust. P.G. is a Wellchild and Royal College of Paediatrics and Child Health Research Fellow.

COMPETING INTERESTS STATEMENT
The authors declare that they have no competing financial interests.

Received 3 November 2003; accepted 9 February 2004
Published online at http://www.nature.com/naturegenetics/

1. Denecke, J. *et al.* Arthrogryposis, renal tubular dysfunction, cholestasis (ARC) syndrome: case report and review of the literature. *Klin. Padiatr.* **212**, 77–80 (2000).
2. Di Rocco, M. *et al.* Arthrogryposis, renal dysfunction and cholestasis syndrome: report of five patients from three Italian families. *Eur. J. Pediatr.* **154**, 835–839 (1995).
3. Eastham, K.M. *et al.* ARC syndrome: an expanding range of phenotypes. *Arch. Dis. Child.* **85**, 415–420 (2001).
4. Horslen, S.P., Quarrell, O.W. & Tanner, M.S. Liver histology in the arthrogryposis multiplex congenita, renal dysfunction, and cholestasis (ARC) syndrome: report of three new cases and review. *J. Med. Genet.* **31**, 62–64 (1994).
5. Abdullah, M.A., Al-Hasnan, Z., Okamoto, E. & Abomelha, A.M. Arthrogryposis, renal dysfunction and cholestasis syndrome. *Saudi Med. J.* **21**, 297–299 (2000).
6. Huizing, M. *et al.* Molecular cloning and characterisation of human VPS18, VPS11, VPS16, and VPS33. *Gene* **264**, 241–247 (2001).
7. Halachmi, N. & Lev, Z. The Sec1 family: a novel family of proteins involved in synaptic transmission and general secretion. *J. Neurochem.* **66**, 889–897 (1996).
8. Jahn, R. & Sudhof, T.C. Membrane fusion and exocytosis. *Annu. Rev. Biochem.* **68**, 863–911 (1999).
9. Rothman, J.E. Mechanisms of intracellular protein transport. *Nature* **372**, 55–63 (1994).
10. Gissen, P. *et al.* ARC syndrome is not allelic to PFIC I and II (meeting abstract). *Eur. J. Hum. Genet.* **11** (s1), 827 (2003).
11. Morgan, N.V. *et al.* A novel locus for Meckel-Gruber syndrome, MKS3, maps to chromosome 8q24. *Hum. Genet.* **111**, 456–461 (2002).
12. Mueller, R.F. & Bishop, D.T. Autozygosity mapping, complex consanguinity, and autosomal recessive disorders. *J. Med. Genet.* **30**, 798–799 (1993).
13. Wang, D.G. *et al.* Large scale identification, mapping and genotyping of single nucleotide polymorphisms in the human genome. *Science* **280**, 1077–1082 (1998).
14. Iwasaki, H. Accuracy of genotyping for single nucleotide polymorphisms by a microarray-based single nucleotide polymorphism typing method involving hybridization of short allele-specific oligonucleotides. *DNA Res.* **9**, 59–62 (2002).
15. Darsow, T., Burd, C.G. & Emr, S.D. Acidic di-leucine motif essential for AP-3-dependent sorting and restriction of the functional specificity of the Vam3p vacuolar t-SNARE. *J. Cell Biol.* **142**, 913–922 (1998).
16. Pond, L. *et al.* A role for acidic residues in di-leucine motif-based targeting to the endocytic pathway. *J. Biol. Chem.* **270**, 19989–19997 (1995).
17. Hanigan, M.H. *et al.* Decreased expression of gamma-glutamyl transpeptidase at the bile canaliculus in arthrogryposis – renal dysfunction - cholestasis syndrome (meeting abstract). *Lab. Invest.* **83**, 301A (2003).
18. Peterson, M.R. & Emr, S.D. The class C Vps complex functions at multiple stages of the vacuolar transport pathway. *Traffic* **2**, 476–486 (2001).
19. Sevrioukov, E.A., He, J.P., Moghrabi, N., Sunio, A. & Kramer, H. A role for the deep orange and carnation eye color genes in lysosomal delivery in Drosophila. *Mol. Cell* **4**, 479–86 (1999).
20. Suzuki, T. *et al.* The mouse organellar biogenesis mutant buff results from a mutation in Vps33a, a homologue of yeast vps33 and Drosophila carnation. *Proc. Natl. Acad. Sci. USA* **100**, 1146–1150 (2003).
21. Gallwit, D. & Jahn, R. The riddle of the Sec1/Munc-18 proteins – new twists added to their interactions with SNAREs. *Trends Biochem. Sci.* **28**, 113–115 (2003).
22. Pevsner, J., Hsu, S.C. & Scheller, R.H. n-Sec1: a neural-specific syntaxin-binding protein. *Proc. Natl. Acad. Sci. USA* **91**, 1445–1449 (1994).
23. Garcia, E.P., Gatti, E., Butler, M., Burton. J. & De Camilli, P. A rat brain Sec1 homologue related to Rop and UNC18 interacts with syntaxin. *Proc. Natl. Acad. Sci. USA* **91**, 2003–2007 (1994).
24. Kim, B.Y. *et al.* Molecular characterization of mammalian homologues of class C Vps proteins that interact with syntaxin-7. *J. Biol. Chem.* **276**, 29393–29402 (2001).
25. Poupon, V., Stewart, A., Gray, S.R., Piper R.C. & Luzio, J.P. The role of mVps18p in clustering, fusion, and intracellular localization of late endocytic organelles. *Mol. Biol. Cell* **14**, 4057–4027 (2003).
26. Cantalupo, G., Alifano, P., Roberti, V., Bruni, C.B. & Bucci, C. Rab-interacting lysosomal protein (RILP): the Rab7 effector required for transport to lysosomes. *EMBO J.* **20**, 683–693 (2000).
27. Caplan, S., Hartnell, L.M., Aguilar, R.C., Naslavsky, N. & Bonifacino, J.S. Human Vam6p promotes lysosome clustering and fusion in vivo. *J. Cell Biol.* **154**, 109–121 (2001).
28. Devonald, M.A.J., Smith, A.N., Poon, J.P., Ihrke, G. & Karet, F.E. Non-polarized targeting of AE1 causes autosomal dominant distal renal tubular acidosis. *Nat. Genet.* **33**, 125–127 (2003).
29. Sambrook, J., Fritsch, E.F. & Maniatis, T. *Molecular Cloning: A Laboratory Manual* 2nd edn. (Cold Spring Harbor Laboratory Press, Cold Spring Harbor, New York, 1989).
30. Johnson, C.A., Padget, K., Austin, C.A. & Turner, B.M. Deacetylase activity associates with topoisomerase II and is necessary for etoposide-induced apoptosis. *J. Biol. Chem.* **276**, 4539–4542 (2001).